Response to Editor comments:
(comments in black font, our responses in blue)

Another revision of the manuscript has helped to further improve presentation and scientific content.
This is also appreciated by the reviewer who, nevertheless, raises a few remaining points that need to be resolved:

(i) The simplistic representation of sedimentary oxygen consumption needs to be acknowledged and the statement that sediment oxygen consumption is important for hypoxia, needs to be adjusted.

Response: As suggested, we have modified the last sentence of the abstract as follows (addition in bold):
"A **model-derived** oxygen budget is presented and **suggests** that sediment oxygen consumption is the dominant oxygen sink below the pycnocline and that advection of oxygen in the bottom waters acts as an oxygen sink in spring…"

In the Discussion we now say:
"The importance of SOC **suggested** by our model is consistent with recent observational studies in the ECS."

(ii) Because you chose to separate interannual from intra-seasonal, time scales under consideration should be expressed more clearly throughout the text (e.g. in line 458-460 you presumably refer to intra-seasonal without mentioning any time scale nor change in forcing at all?). Right now the conclusions on intra-seasonal time scales are not overly strong, which might be due to a lack of clarity and an implicit association of variability with interannual variability. I do not ask for a new analysis, but for a more careful presentation.

Response: We have abandoned the term intra-seasonal (apparently it was misunderstood as interseasonal by Reviewer 3) and instead now use short-term variability (defined as variability on scales of days to weeks). We hope this minimizes the risk of confusion about timescales. We have reassessed the entire manuscript and have clarified the text on lines 458 – 460 by explicitly stating when we are talking about interannual and short-term variability as follows (additions to the text in bold):

*"In section 3.2.1 above, **where we discussed interannual variability**, we noted that while the years 2010 and 2012 had very similar FW input and DIN load, 2010 had a much larger hypoxic area. Likewise, the years 2009 and 2013 were very similar in terms of FW input and DIN load, but 2009 had a much larger hypoxic area. It now becomes obvious that the frequency and severity of high-wind events**, i.e. variations on short timescales**, explains the **interannual** differences in both cases."*

minor issues:

line 74 please use SI units for O2 concentrations

Response: The unite mg L^{-1} is commonly used in the coastal hypoxia literature and hypoxia criteria are commonly defined using this unit (e.g. 2 mg L^{-1} or 3 mg L^{-1}). Because of the familiarity that readers of coastal hypoxia literature have with these criteria and the unit, we would prefer to leave it as it is. However, if the Editor insists, we can change it to x1000 mg m^{-3}, but we'd much prefer to leave it as is.

Fig 7 and Table 1 assume zero lag. Would be interesting to know whether the consideration of a lag led to significant changes.

Response: Consideration of lags does neither increase the correlation coefficient nor decrease the variability around the best fit.

l. 362 correlation coefficients should be expressed as 0.43 , not 43 % etc.

Response: We changed to decimal notation throughout the manuscript.

I hope that these remaining changes can be dealt with without too much trouble and look forward to receiving a suitably revised manuscript.

Response:
Thank you for these constructive suggestions.

Response to comments by Reviewer #3:
(comments in black font, our responses in blue)

I want to thank the authors for their answers to my comments, and their actions they have taken in the manuscript. By removing figure 8 (in the last version of the manuscript), and adding some text which helps the reader to follow the logics of the study, it makes it easier to follow.

Despite this, I still do think that it is quite difficult to follow the logics behind the presentation of the results. This is mainly a result of the choice of figure composition and the related text, and that different timescales are mixed up (the manuscript is dealing with interdaily, intraseasonal and interannual timescales). Below I'm giving some suggestions of improvement. Some of them will be repetitions of comments in the previous round that I wish to clarify.

1. Regarding my comment number 1 on putting your study in perspective to previous studies on the same topic:

Thank you for adding the last paragraph in the introduction. To make it even clearer, you could write something like: "In contrast to previous studies on the same topic, we here address a larger number of factors driving hypoxic variability, including xxx,xxx,xxx. Additionally we address longer time scales".

Response: We prefer to use our present formulation.

Here I also have an important remark : You state in the manuscript that your study shows that sediment oxygen consumption is important for hypoxia. I think that you should be careful with this, and rather write that your model simulations **suggest** that sediment oxygen consumption is important. The reasons behind this are that your parameterization of sediment oxygen consumption is very simple (instant remineralization), and also that you have not provided a thorough evaluation of its performance. The comparison that you provide in the discussion, of your modelled sediment oxygen consumption with what has been measured in a few studies, is not enough to state this.

Response: We modified the last sentence of the abstract accordingly as follows (addition in bold):
"A **model-derived** oxygen budget is presented and **suggests** that sediment oxygen consumption is the dominant oxygen sink below the pycnocline and that advection of oxygen in the bottom waters acts as an oxygen sink in spring…"

In the Discussion we now say:
"The importance of SOC **suggested** by our model is consistent with recent observational studies in the ECS."

2. Regarding my comment on focusing on one time scale:

In my opinion, the finding in section 3.2.3 that is relevant to section 3.2.1 is about interannual variability, not intraseasonal variability. You are explaining the difference in the hypoxic extent between 2010 and 2012 by the interannual variability in frequency and severity of high wind events. Even though these act on shorter time scales, there is an interannual signal in this

process. To me it sounds wrong to state that intraseasonal variability affects interannual variability. This is one of the main reasons why I find your manuscript difficult to follow. Intraseasonal variability is by definition how something varies over seasons.

On the other hand, processes that are acting on shorter time scales, such as strong wind events (and also marine primary production), can be important for the interannual variability.

Response: The appears to be a misunderstanding about the term **intra-**seasonal, which means within a season (in this case referring to within the hypoxic season), as opposed to **inter**seasonal (from season to season), which is not what we mean but this seems to be what the Reviewer has interpreted the term to mean. We have now replaced the term intra-seasonal with short-term throughout the manuscript and define short-term variability as variability on time scales of days to weeks. We are in agreement with the Reviewer on our finding that short-term wind events can produce interannual variability – this is exactly one of the important points we hope to have shown. Hopefully using the term short-term variability has made the manuscript easier to follow.

In the last report I stated that I do not think that section 3.2.2 adds any new to the story. I still think that this is the case. When you look at daily timescales , you find a weaker correlation between biological rates and oxygen concentration than when looking on interannual timescales, and you use this to argue that physical processes must be important, which leads to section 3.2.3. **(Please note that when plotting daily means as you do in figure 7 you are dealing with daily timescales, not intraseasonal timescales as you state in the title of the subsection.) .** But then in subsection 3.2.3 you partly go back to interannual variability. Both in figure 9 and 10 you look at variations between years. In fact, you do not need figure 7 to argue that physical processes are important, you can already see in figure 5 (and also the budget) that there are other processes than biology that is important. \

If you want to keep both timescales, you have to be clear in their separation, and also be careful to use the right terms (i.e. not interseasonal when you are talking about interdaily).

To make it simple, I would recommend to focus on interannual timescales (I think that you have a very nice story there).

Response: As per our previous response, the reviewer clearly is confused about the term **intra-**seasonal, which means within a season, as opposed to **interseasonal** (from season to season), which is not what we mean. We hope that by abandoning the term intra-seasonal variability and instead using short-term variability defined as days to weeks has resolved these issues to the satisfaction of Reviewer and made it clearer for future readers as well.

3. Regarding the suggestion about including budgets for different years:

I think that I was not clear with what I meant here. The idea was that if you look into budget for different years (rather than different months), you might be able to separate the roles played by the stratification (i.e. the freshwater plume) on the vertical supply on oxygen, and on the primary production, respectively, on the interannual variability on hypoxia. I know that you have plotted the budgets for different years in figure 11. But as it is shown now it is impossible to make a link to the interannual variability of hypoxia.

Again, this is a question about what timescale you want to focus on in the manuscript. As it is now, figure 11 is about intraseasonal variability (i.e. variations over seasons).

Response: No further action taken.

A numerical model study of the main factors contributing to hypoxia and its interannual and short-term variability in the East China Sea

Haiyan Zhang[1, 2], Katja Fennel[1,*], Arnaud Laurent[1], Changwei Bian[3]

[1]Department of Oceanography, Dalhousie University, Halifax, Nova Scotia, Canada

[2]School of Marine Science and Technology, Tianjin University, Tianjin, China

[3] Physical Oceanography Laboratory/CIMST, Ocean University of China, and Qingdao National Laboratory for Marine Science and Technology, Qingdao, China

*Corresponding author

Abstract

A three-dimensional physical-biological model of the marginal seas of China was used to analyze interannual and intra-seasonal variations in hypoxic conditions and identify the main processes controlling their generation off the Changjiang Estuary. The model was compared against available observations and reproduces the observed temporal and spatial variability of physical and biological properties including bottom oxygen. Interannual variations of hypoxic extent in the simulation are partly explained by variations in river discharge but not nutrient load. As riverine inputs of freshwater and nutrients are consistently high, promoting large productivity and subsequent oxygen consumption in the region affected by the river plume, wind forcing is important in modulating interannual and short-term variability. Wind direction is relevant because it determines the spatial extent and distribution of the freshwater plume which is strongly affected by either upwelling or downwelling conditions. High-wind events can lead to partial reoxygenation of bottom waters and, when occurring in succession throughout the hypoxic season, can effectively suppress the development of hypoxic conditions thus influencing interannual variability. A model-derived oxygen budget is presented and suggests that sediment oxygen consumption is the dominant oxygen sink below the pycnocline and that advection of oxygen in the bottom waters acts as an oxygen sink in spring but becomes a source during hypoxic

Deleted: intra-seasonal

Deleted: off

Deleted: Changjiang Estuary

Deleted: intra-seasonal

Deleted: n

Deleted: shows

conditions in summer, especially in the southern part of the hypoxic region, which is influenced by open-ocean intrusions.

1. Introduction

In coastal seas, hypoxic conditions (oxygen concentrations lower than 2 mg L^{-1} or 62.5 mmol m^{-3}) are increasingly caused by rising anthropogenic nutrient loads from land (Diaz & Rosenberg, 2008; Rabalais et al., 2010; Fennel and Testa, 2019). Hypoxic conditions are detrimental to coastal ecosystems leading to a decrease in species diversity and rendering these systems less resilient (Baird et al., 2004; Bishop et al., 2006; Wu, 2002). Hypoxia is especially prevalent in coastal systems influenced by major rivers such as the northern Gulf of Mexico (Bianchi et al., 2010), Chesapeake Bay (Li et al., 2016), and the Changjiang Estuary (CE) in the East China Sea (Li et al., 2002).

The Changjiang is the largest river in China and fifth largest in the world in terms of volume transport, with an annual discharge of 9×10^{11} m^3 $year^{-1}$ via its estuary (Liu et al., 2003). The mouth of the CE is at the confluence of the southeastward Yellow Sea Coastal Current and the northward Taiwan Warm Current (Figure 1). Hydrographic properties in the outflow region of the CE are influenced by several different water masses including fresh Changjiang Diluted Water, relatively low-salinity coastal water, more saline water from the Taiwan Warm Current, and high-nutrient, low-oxygen water from the subsurface of the Kuroshio (Wei et al., 2015; Yuan et al., 2008). The interactions of these water masses together with wind forcing and tidal effects lead to a complicated and dynamic environment.

Freshwater (FW) discharge by the Changjiang reaches its minimum in winter when the strong northerly monsoon (dry season) prevails and peaks in summer during the weak southerly monsoon (wet season) resulting in a large FW plume adjacent to the estuary. Along with the FW, the Changjiang delivers large quantities of nutrients to the East China Sea (ECS) resulting in eutrophication in the plume region (Li et al., 2014; Wang et al., 2016). Since the 1970s, nutrient load has increased more than twofold with a subsequent increase in primary production (PP) in the outflow region of the estuary (Liu et al., 2015). Hypoxia off the CE was first detected in 1959 and, with a spatial extent of up to 15,000 km^2, is among the largest coastal hypoxic zones in the world (Fennel & Testa, 2019). Although no conclusive trend in oxygen minima has been observed (Wang, 2009; Zhu et

al., 2011), hypoxic conditions are suspected to have expanded and intensified in recent decades (Li et al., 2011; Ning et al., 2011) due to the increasing nutrient loads from the Changjiang (Liu et al., 2015).

It is generally accepted that water-column stratification and the decomposition of organic matter are the two essential factors for hypoxia generation, and this is also the case for the shelf region off the CE (Chen et al., 2007; Li et al., 2002; Wei et al., 2007). High solar radiation and FW input in summer contribute to strong vertical stratification which is further enhanced by near-bottom advection of waters with high salinities (> 34) and low temperatures (< 19 °C) by the Taiwan Warm Current. The resulting strong stratification inhibits vertical oxygen supply (Li et al., 2002; Wang, 2009; Wei et al., 2007). At the same time, high organic matter supply fuels microbial oxygen consumption in the subsurface (Li et al., 2002; Wang, 2009; Wei et al., 2007; Zhu et al., 2011). It has also been suggested that the Taiwan Warm Current brings additional nutrients contributing to organic matter production (Ning et al., 2011) and that the low oxygen concentrations (~ 5 mg L^{-1}) of the Taiwan Warm Current precondition the region to hypoxia (Ning et al., 2011; Wang, 2009).

While observational analyses suggest that hypoxia off the CE results from the interaction of various physical and biogeochemical processes, quantifying the relative importance of these processes and revealing the dynamic mechanisms underlying hypoxia development and variability require numerical modeling (Peña et al., 2010). Numerical modeling studies have proven useful for many other coastal hypoxic regions such as the Black Sea northwestern shelf (Capet et al., 2013), Chesapeake Bay (Li et al., 2016; Scully, 2013), and the northern Gulf of Mexico (Fennel et al., 2013; Laurent & Fennel, 2014).

Models have also been used to study the hypoxic region of the CE. Chen et al. (2015a) used a 3D circulation model with a highly simplified oxygen consumption parameterization (a constant consumption rate) to investigate the effects of physical processes, i.e. FW discharge, and wind speed and direction, on the dissipation of hypoxia. Chen et al. (2015b) examined the tidal modulation of hypoxia. The model domain in these two previous studies was relatively limited encompassing only the CE, Hangzhou Bay and the adjacent coastal ocean but did not cover the whole area affected by hypoxia (Wang, 2009; Zhu et al., 2011). Zheng et al. (2016) employed a nitrogen cycle model coupled with a 3D hydrodynamic model to examine the role of river discharge, wind speed and direction on hypoxia, and

also emphasized the physical controls. These previous modeling studies focused on the response of hypoxia to physical factors only and did not address seasonal evolution and interannual variations of hypoxia or the influence of variability in biological rates.

More recently, Zhou et al. (2017) analyzed the seasonal evolution of hypoxia and the importance of the Taiwan Warm Current and Kuroshio intrusions as a nutrient source using an advanced coupled hydrodynamic-biological model. However, the baseline of their model does not include sediment oxygen consumption (SOC), which is thought to be a major oxygen sink in the hypoxic region off the CE (Zhang et al., 2017) and other river-dominated hypoxic regions including the northern Gulf of Mexico (Fennel et al. 2013, Yu et al. 2015a,b). Zhou et al. (2017) acknowledged the importance of SOC based on results from a sensitivity experiment but did not quantify its role in hypoxia generation.

Here we introduce a new 3D physical-biological model implementation for the ECS that explicitly includes nitrogen and phosphorus cycling and SOC. The model is a new regional implementation for the ECS of an existing physical-biogeochemical model framework that has been extensively used and validated for the northern Gulf of Mexico (Fennel et al., 2011, 2013; Laurent et al., 2012; Laurent and Fennel, 2014; Yu et al., 2015b; Fennel and Laurent, 2018). The hypoxic zones in the northern Gulf of Mexico and off the CE have similar features including the dominant influence of a major river (Changjiang and Mississippi), a seasonal recurrence every summer, a typical maximum size of about 15,000 km^2, documented P-limitation following the major annual discharge in spring and a significant contribution of SOC to oxygen sinks in the hypoxic zone (Fennel and Testa 2019).

We performed and assessed a 6-year simulation of the ECS and use the model results here to identify the main factors driving hypoxia variability on interannual and short-term (days to seasons) timescales in the simulation. More specifically, we investigate the role of interannual variations in riverine inputs of nutrients and FW versus short-term variations in coastal circulation and mixing. We also present an oxygen budget to quantify the relative importance of SOC and the influence of lateral advection of oxygen in the model. The companion study by Grosse et al. (2020) used the same model to quantify the importance of intrusions of nutrient-rich oceanic water from the Kuroshio for hypoxia development off the CE.

Deleted: ,

Deleted: intra-seasonal

Deleted: intra-seasonal

Deleted: A

Deleted: s

2. Model description

2.1. Physical model

The physical model is based on the Regional Ocean Modeling System (ROMS; Haidvogel et al., 2008) and was implemented for the ECS by Bian et al. (2013a). The model domain extends from 116°E to 134°E and 20°N to 42°N (Figure 1), covering the Bohai Sea, the Yellow Sea, the ECS, part of the Japan Sea and the adjacent northwest Pacific, with a horizontal resolution of 1/12° (about 10 km) and 30 vertical layers with enhanced resolution near the surface and bottom. The model uses the recursive Multidimensional Positive Definite Advection Transport Algorithm (MPDATA) for the advection of tracers (Smolarkiewicz and Margolin, 1998), a third-order upstream advection of momentum, and the Generic Length Scale (GLS) turbulence closure scheme (Umlauf & Burchard, 2003) for vertical mixing.

The model is initialized with climatological temperature and salinity from the World Ocean Atlas 2013 V2 (WOA13 V2) (Locarnini et al., 2013; Zweng et al., 2013), and is forced by 6-hourly wind stress, and heat and FW fluxes from the ECMWF ERA-Interim dataset (Dee et al., 2011). Open boundary conditions for temperature and salinity are prescribed from the monthly climatology (WOA13 V2), and horizontal velocities and sea surface elevation at the boundaries are specified from the monthly SODA data set (Carton & Giese, 2008). In addition, eight tidal constituents (M2, S2, N2, K2, K1, O1, P1 and Q1) are imposed based on tidal elevations and currents extracted from the global inverse tide model TPXO7.2 of Oregon State University (OSU, Egbert & Erofeeva, 2002). At the open boundaries, Chapman and Flather conditions are used for free surface and barotropic velocities, respectively, and the radiation condition for the baroclinic velocity. Eleven rivers are included in the model. FW discharge from the Changjiang uses daily observations from the Datong Hydrological Station (DHS; www.cjh.com.cn). Since daily observations are not available for the other rivers, we prescribed monthly or annual climatologies (Liu et al., 2009; Tong et al., 2015; Zhang, 1996).

Deleted: used in this study

Deleted: from

Deleted: data set of

Deleted: the

Deleted: the

Deleted: y

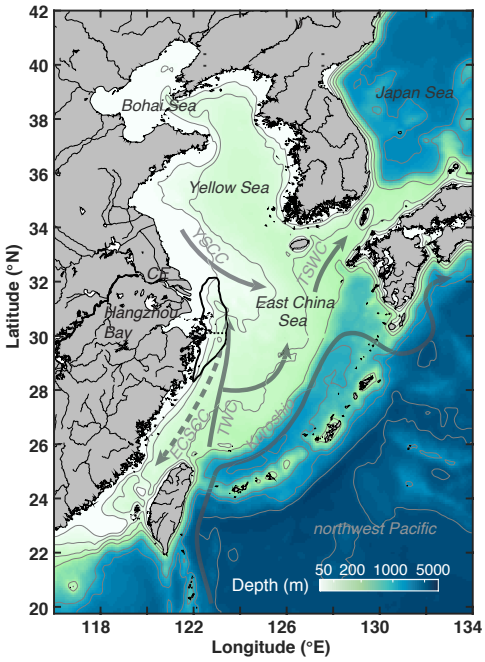

Figure 1. Bathymetry of the model domain with 30, 50, 100, 200, 1000, 2000 and 5000 m isobaths. The black outline near the Changjiang Estuary (CE) and Hangzhou Bay indicates the zone typically affected by low-oxygen conditions (dotted line shows separation between northern and southern zones). Solid grey arrows denote currents present throughout the year (Kuroshio; TWC: Taiwan Warm Current; YSCC: Yellow Sea Coastal Current). The dashed grey arrow indicates the direction of the wintertime East China Sea Coastal Current (ECSCC) which flows in the opposite direction in summer.

Deleted: to

Deleted: time flow

2.2. Biological model

The biological component is based on the pelagic nitrogen cycle model of Fennel et al. (2006, 2011, 2013) and was extended to include phosphate (Laurent et al., 2012; Laurent & Fennel, 2014) and riverine dissolved organic matter (Yu et al., 2015b). The model includes two forms of dissolved inorganic nitrogen (DIN), nitrate (NO3) and ammonium (NH4), phosphate (PO4), phytoplankton (Phy), chlorophyll (Chl), zooplankton (Zoo), two pools of detritus, suspended and slow-sinking small detritus (SDet) and fast-sinking large

detritus (LDet), and riverine dissolved organic matter (RDOM). Here, riverine dissolved and particulate organic nitrogen enter the pools of RDOM and SDet, respectively. The remineralization rate of RDOM is an order of magnitude lower than that of SDet to account for the more refractory nature of the riverine dissolved organic matter (Yu et al., 2015b).

At the sediment-water interface, SOC is parameterized assuming "instantaneous remineralization," i.e. all organic matter reaching the sediment is remineralized instantaneously and oxygen is consumed due to nitrification and aerobic remineralization at the same time. In the "instantaneous remineralization", all phosphorus is returned to the water column as PO4 while a constant fraction of fixed nitrogen is lost due to denitrification. All biogeochemical model parameters are given in Table S1 in the Supplement. A more detailed model descriptions can be found in the Supplement to Laurent et al. (2017).

Light is vertically attenuated by chlorophyll, detritus and seawater itself. In addition, to account for the effects of colored dissolved organic matter (CDOM) and suspended sediments, which show relatively high values near the coast and in the river plume (Bian et al., 2013b; Chen et al., 2014), a light-attenuation term dependent on water depth and salinity is introduced which yields higher attenuation in shallow areas and in the FW plume.

Initial and boundary conditions for NO3, PO4 and oxygen are prescribed using the World Ocean Atlas 2013 (WOA13) climatology (Garcia et al., 2013a,b). A small positive value is used for the other variables. NO3 is nudged towards climatology in the northwest Pacific at depth > 200 m. Monthly nutrient loads of NO3 and PO4 from the Changjiang are from the Global-NEWs Model (Wang et al., 2015) but were adjusted by multiplicative factors of 1.20 and 1.66, respectively, to ensure a match between simulated and observed nutrient concentrations in the CE (see July and Aug 2012 in Figure 2). Nutrient loads in other rivers are based on other published climatologies (Liu et al., 2009; Tong et al., 2015; Zhang, 1996). Due to a lack of data on organic matter loads, river load concentrations of SDet and LDet and RDOM were assumed conservatively at 0.5, 0.2 and 15 mmol N m^{-3}, respectively.

We performed an 8-year simulation from 1 January 2006 to 31 December 2013, with 2006-2007 as model spin up and 2008-2013 used for analysis. Model output was saved daily.

3. Results

3.1. Model validation

Model output is compared with observations of simulated surface and bottom temperature, salinity, current patterns and strength, surface chlorophyll, surface nitrate and bottom oxygen. The model reproduces remotely sensed spatial and temporal SST patterns (NOAA AVHRR) very well (Figure S1) with an overall correlation coefficient, i.e. considering all climatological monthly mean SST fields interpolated to the model grid, of 0.98. Simulated surface and bottom salinity also show similar spatial and seasonal patterns as available *in situ* observations (Figures S2 and S3) with overall correlation coefficients, i.e. using all surface and all bottom data points, of 0.77 and 0.84, respectively. Simulated surface and bottom temperature, when compared with available *in situ* data (Figures S4 and S5), are also consistent with the observations with overall correlation coefficients of 0.96 and 0.93.

The simulated current systems in the ECS and YS show typical seasonal variations as follows (see also Figure S6). In winter, currents mainly flow southward on the Yellow Sea and ECS shelves driven by the northerly wind. In contrast, the ECS Coastal Current and the Korean Coastal Current flow northward in summer. The Kuroshio is stronger in

Deleted: East China Sea

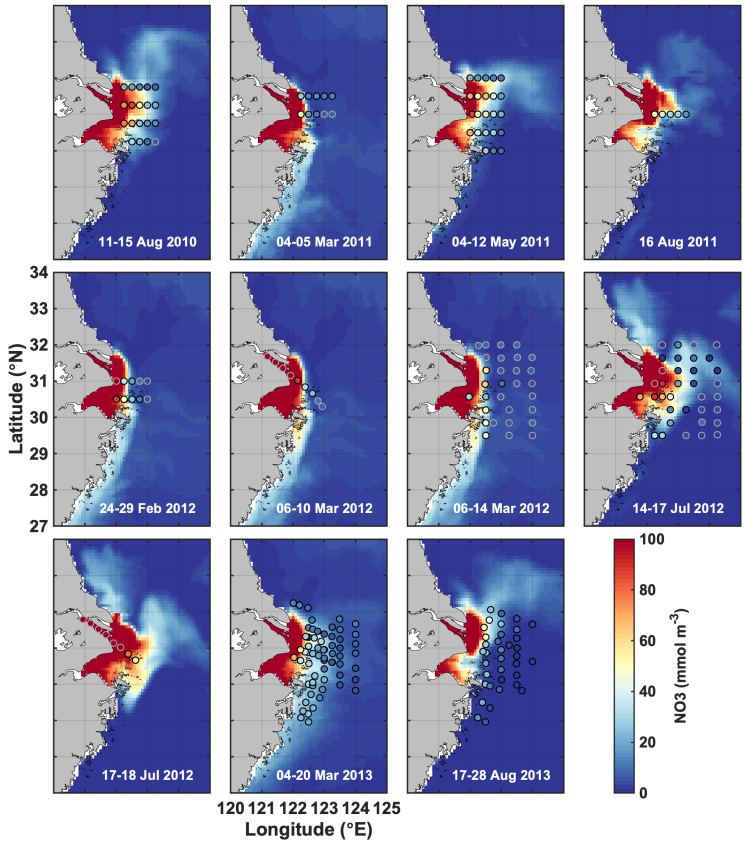

Figure 2: Simulated surface nitrate (colored map) shown for the day that marks the mid-point of the cruise dates (given in each panel) the compared to observations (dots) during 11 cruises from 2011 to 2013.

summer than in winter. The model captures the seasonal pattern of the current system and resolves currents in the ECS and Yellow Sea (also see Grosse et al. 2020).

Simulated monthly averaged (2008-2013) surface chlorophyll concentrations in May, August and November are compared with satellite-derived fields (MODIS-Terra) and agree well with spatial correlation coefficients of 0.77, 0.94 and 0.64, respectively (Figure S7).

241 Simulated surface nitrate concentrations are shown in comparison to *in situ* observations
242 in Figure 2 and agree well with an overall correlation coefficient of 0.84. Observations in
243 March and July of 2012 show strongly elevated concentrations in the CE and a sharp
244 gradient in the vicinity of the estuary's mouth that are well represented by the model.
245 Likewise, simulated and observed bottom oxygen distributions are compared in Figure 3
246 and agree reasonably well overall with an overall correlation coefficient of 0.71 although
247 the model underestimates observed low-oxygen conditions in July of 2011 and 2013 and
248 August 2013.
249 Together, these comparisons show that the model is able to reproduce important aspects
250 of the physical-biogeochemical dynamics in the study region.

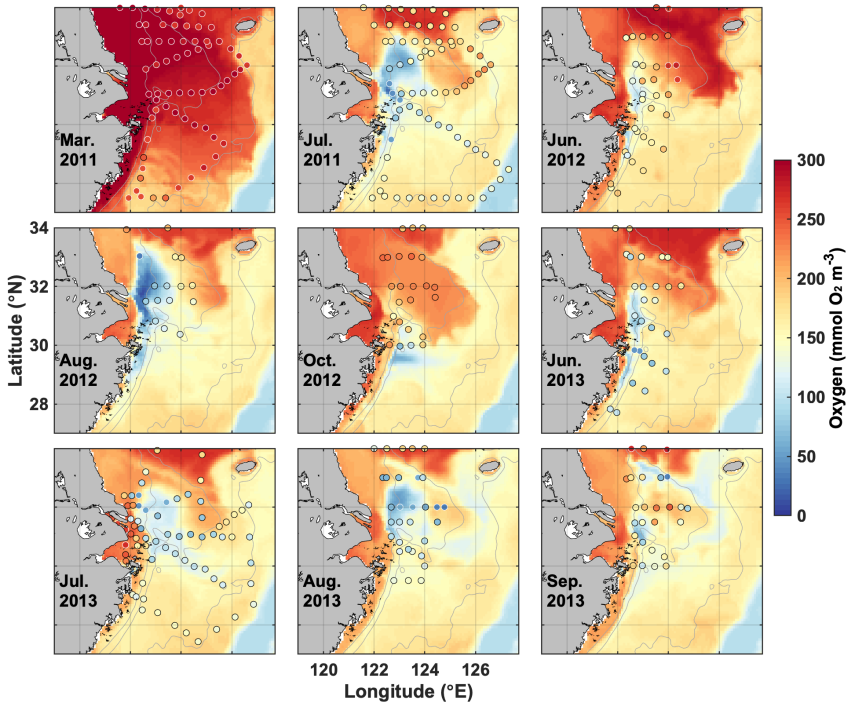

Figure 3. Simulated bottom oxygen (colored map) shown for the day that marks the mid-point of the cruise dates compared with observations (dots) during nine cruises from 2011 to 2013.

251

3.2. Simulated oxygen dynamics

First, we describe the timing and distribution of simulated bottom-water oxygen off the CE to set the stage for our investigation into the drivers underlying hypoxia variability. The model simulates annually recurring hypoxic conditions with a typical seasonal cycle where bottom waters are well-oxygenated until April/May, hypoxic conditions establish in June or July, become more pronounced in August, and disperse in October or November (Figure 4a, c). However, the model also simulates significant interannual variability in timing and extent of hypoxia over the 6-year simulation period (Figure 4b, c). The years with largest maximum hypoxic extent are 2010 (20,520 km^2), 2009 (16,660 km^2), 2012 (13,930 km^2) and 2008 (12,720 km^2) while the simulated hypoxic extent is much smaller (<5,000 km^2) in 2011 and 2013. The ranking is similar when considering the time-integrated hypoxic extent (Figure 4b). The year with the largest maximum and integrated hypoxic extent

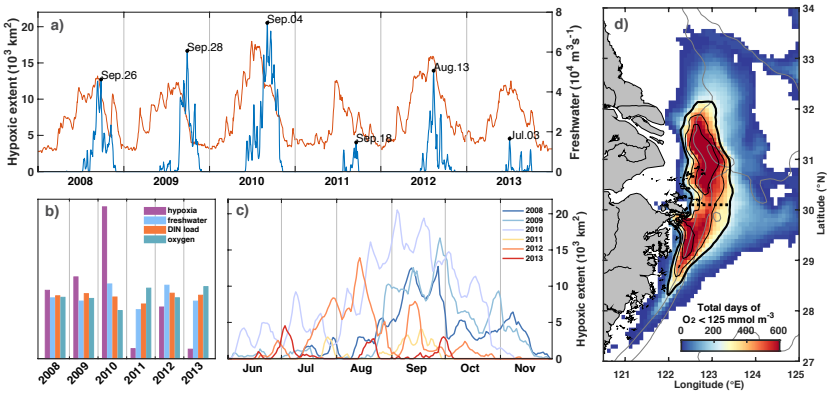

Figure 4. a) Time series of freshwater discharge (thin red line) and simulated hypoxic extent (thick blue line) with peaks specified by date. b) Annual comparison of normalized time-integrated hypoxic extent, freshwater discharge, and DIN load, and summer-mean bottom oxygen concentration. c) Evolution of simulated hypoxic extent by year. d) Frequency map of number of days when bottom oxygen concentrations were below 125 mmol m^{-3} (4 mg/l). The black isolines indicate 240, 360 and 480 days (or 40, 60 and 80 days per year). The thick solid line indicates the region we refer to as the typical low-oxygen zone and the dashed line shows the demarcation between its northern and southern regions.

(2010) also has the highest peak discharge (Figure 4a) and highest annual FW discharge (65,400 m^3 s^{-1}), although the annual discharge in 2008 and 2012 is not much smaller than in 2010.

The region where low-oxygen conditions are most commonly simulated is indicated by the frequency map in Figure 4d, which shows the total number of days in the 6-year simulation when bottom oxygen concentrations were below 125 mmol m^{-3} (or 4 mg/l), i.e. twice the hypoxic threshold. It is known from observations that there are two centers of recurring hypoxic conditions: the northern core is located just to the east of the CE and Hangzhou Bay and the southern core to the southeast of Hangzhou Bay. The model is consistent with these observations and simulates two distinct core regions of low-oxygen conditions centered at 31°N and 29.3°N. The northern core region is larger than the southern core region (9,050 km^2 for a threshold of 80 days per year of < 4 mg/l compared to 5,230 km^2). We will refer to the region defined by a threshold of 40 days of < 4 mg/l of per year (solid black line in Figure 1 and 4d) as the "typical low-oxygen zone" for the remainder of the manuscript and demarcate the northern and southern sections by 30.1°N latitude (dashed line in Figures 1 and 4d).

There are marked differences in the phenology of simulated hypoxic extent (Figure 4c). Among the four years with largest hypoxic areas, hypoxia establishes relatively late (mid-August) and lasts long (into November) in 2008 and 2009. In contrast in 2012, hypoxic conditions establish earlier (June), are most pronounced in August and are eroded by mid-October. In 2010, the year with the largest peak extent, hypoxia establishes already at the beginning of June and is maintained until the end of October, leading to the largest time-integrated hypoxia by far among the 6 years (Figure 4b). In all years there are times when hypoxic extent decreases rapidly.

In the following sections, we explore the drivers underlying these interannual and short-term variations, specifically the contribution of year-to-year variations in nutrient loads and FW inputs from the Changjiang, and the potential reasons for shorter-term variability in hypoxia by assessing the role of biological processes and physical forcing.

Deleted: intra-seasonal

Deleted: intra-seasonal

297 *3.2.1 Interannual variations in hypoxia*

298 The first question we address is: Do year-to-year variations in nutrient load and FW input
299 from the Changjiang explain interannual variability in hypoxic conditions? We do this by
300 investigating correlations of time-integrated hypoxic area, average PP, total oxygen
301 consumption (OC) by respiration, SOC, and bottom oxygen in the typical low-oxygen zone
302 (Figure 5 a-f). We also consider the correlation between the spatial extent of the FW plume,
303 defined as the horizontal extent of surface water with salinity less than 29, and annually
304 integrated FW input and DIN load (Figure 5 g-i).

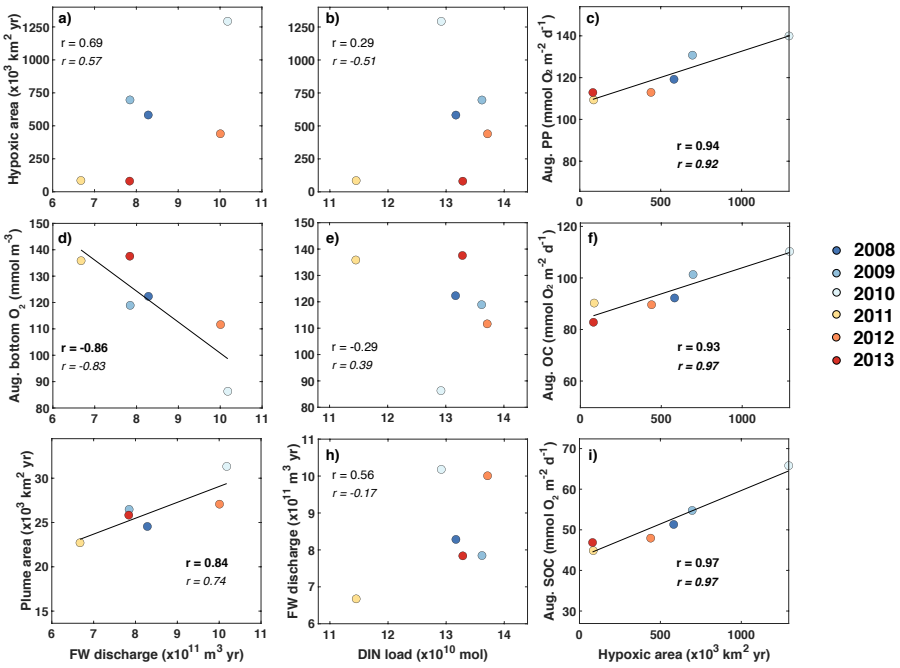

Figure 5. Correlations of time-integrated hypoxic area, average primary production, respiration and bottom oxygen in the typical low-oxygen zone in August, and the spatial extent of the FW plume (defined here as the area with surface salinity smaller than 29) with annually integrated FW input and DIN load. Correlation coefficients are given for all 6 years and, in italic font, after excluding year 2011. Significant correlations are shown in bold font and linear regressions indicated by the black line whenever the correlation is significant at $p<0.05$.

There is a significant negative correlation between annual FW input and mean bottom-water oxygen concentration in the low-oxygen zone of -0.86 and a weaker, statistically insignificant positive correlation of 0.69 between annual FW input and integrated hypoxic area (Figure 5a, d). This indicates that variations in FW input at least partly explain variability in hypoxic conditions. Perhaps surprisingly, there is no convincing correlation between annual FW input and annual DIN load (Figure 5h). Although the correlation coefficient is 0.56 when all 6 years are considered, the correlation reverses to -0.17 when the low-flow year 2011 is excluded and neither of these correlations is statistically significant. As expected, there is a strong positive correlation of 0.84 between the annual FW input and time-integrated plume area (Figure 5g). Plume area can thus be interpreted as a proxy of FW input.

In contrast to the positive correlations between FW input and hypoxia, and FW input and bottom oxygen, correlations between the annual DIN load with integrated hypoxic area and mean bottom-water oxygen are much weaker and insignificant (Figure 5b, e). This implies that interannual variations in DIN load do not lead to year-to-year variations in hypoxia. However, the correlations between integrated hypoxic area and mean rates of PP and OC (especially SOC) in August are significant and strong at 0.94 and 0.93 (0.97), respectively (Figure 5c, f, i). The high correlation between hypoxic area and OC is primarily driven by SOC. Clearly, biological processes are important drivers of hypoxia and contribute to its interannual variability, but they do not appear to result from variations in DIN load. More relevant are variations in FW load, which explain interannual variations in hypoxia at least partly.

Other factors than riverine inputs of nutrients and FW must be contributing to interannual variations. For example, the years 2010 and 2012 both had very similar FW input and DIN load but differed in severity of hypoxia (Figure 5a, b). Likewise, the years 2009 and 2013 were very similar in terms of FW input and DIN load, but very different in hypoxic extent. Next, we investigate the potential reasons for shorter-term variability in hypoxia, i.e. the processes leading to the differences in hypoxia phenology in Figure 4c.

Deleted: %
Deleted: %
Deleted: %
Deleted: %
Deleted: %
Deleted: %
Deleted: %
Deleted: Clearly, o
Deleted: intra-seasonal

3.2.2 Biological drivers of short-term variability in hypoxia

In the previous subsection, we identified biological rates as important drivers of low-oxygen conditions on interannual timescales but unrelated to variations in riverine DIN load. Here we attempt to elucidate what drives variations in biological rates and low-oxygen conditions on shorter timescales by addressing the following two questions. Do low-oxygen conditions correlate with biological rates on these shorter timescales? If yes, what drives variations in biological rates?

For this analysis it seems prudent to distinguish between the northern and southern hypoxic regions for the following reasons. The bathymetry in the northern zone is slightly deeper than in the southern zone (median depth of 28.5 m versus 24.6 m) and several biological rates with direct relevance to oxygen dynamics are different between the two zones (Figure 6). During the summer months (June to September), PP, oxygen consumption in the water column (WOC=OC-SOC), and SOC are larger in the northern zone with medians of 124 compared to 77.0 mmol O_2 m^{-2} d^{-1} for PP, of 43.1 versus 35.9 mmol O_2 m^{-2} d^{-1} for WOC, and 49.3 versus 27.3 mmol O_2 m^{-2} d^{-1} for SOC. During hypoxic conditions, PP and SOC are also notably larger in the northern zone with medians of 151 versus 107 mmol O_2 m^{-2} d^{-1} for PP and 69.9 versus 50.4 mmol O_2 m^{-2} d^{-1} for SOC. In the water column, the difference is reversed and WOC larger in the southern than the northern zone (52.9 versus 46.7 mmol O_2 m^{-2} d^{-1}). Because of these different characteristics, we consider the northern and southern zones of the typical low-oxygen region separately.

First, we explore whether significant relationships exist between daily biological rates and bottom-water oxygen by determining the correlations of daily averaged rates of PP, OC and SOC with daily mean bottom oxygen concentration (Figure 7 and Table 1).

Deleted: *intra-seasonal*

Deleted: intra-seasonal

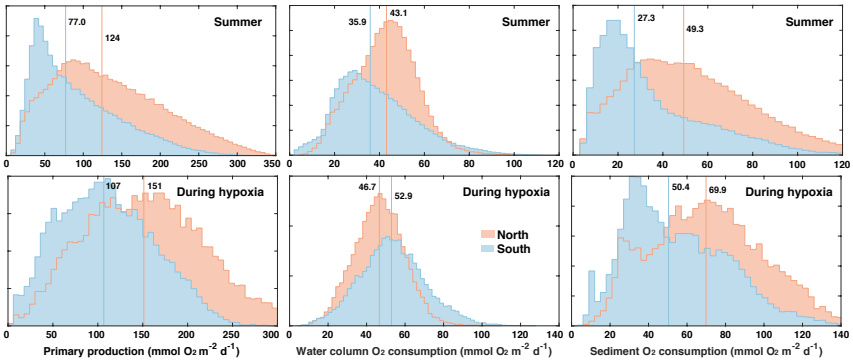

Figure 6: Histograms primary production and water-column and sediment respiration during the summer months (June to September) and during hypoxic conditions in the northern and southern parts of the typically hypoxic zone. Medians are indicated by vertical lines.

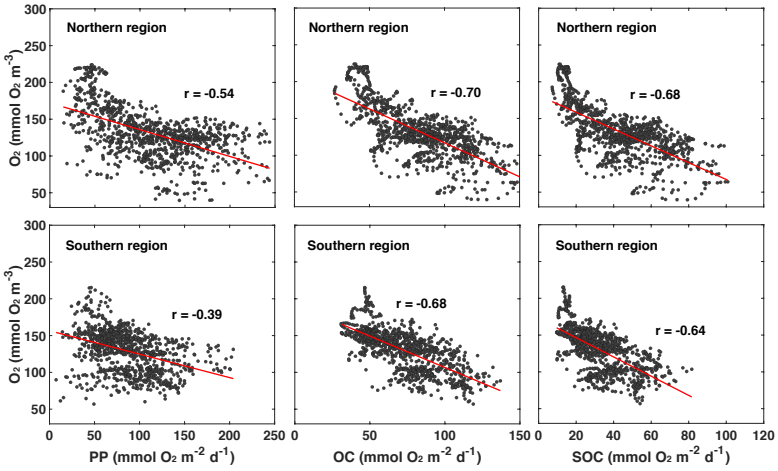

Figure 7. Correlations of daily averaged rates of PP, OC and SOC plotted with daily mean bottom oxygen concentration in the northern and southern regions of the low-oxygen zone in summer. The correlations are all significant. Correlation coefficients and slope and intercept of linear regressions (indicated by red lines) are given in Table 1.

Relationships between bottom oxygen (mmol m^{-3}) in northern region and											
PP (mmol O_2 m^{-2} d^{-1})			OC (mmol O_2 m^{-2} d^{-1})			SOC (mmol O_2 m^{-2} d^{-1})					
r	a	b	r	a	b	r	a	b			
-0.54	-0.36	172	-0.70	-0.92	209	-0.68	-1.14	181			
Same for the southern region											
-0.39	-0.32	157	-0.68	-0.85	192	-0.64	-1.30	172			
Relationships between plume area (10^3 km^2; defined by surface salinity < 29) in northern region											
PP (mmol O_2 m^{-2} d^{-1})			OC (mmol O_2 m^{-2} d^{-1})			SOC (mmol O_2 m^{-2} d^{-1})			Bottom oxygen (mmol m^{-3})		
0.62	6.04	47.6	0.49	2.48	57.7	0.51	2.05	22.0	-0.56	-3.74	171
Same for the southern region											
0.43	3.78	64.6	0.56	3.18	57.8	0.43	1.50	24.7	-0.49	-3.52	149

Table 1. Correlation coefficients and parameters of a linear model fit (of the form y=ax+b) between

Indeed, daily PP, OC, and SOC are all significantly and negatively correlated with bottom-water oxygen. This confirms that local production of organic matter and the resulting biological oxygen consumption are important for hypoxia development and that variations in these rates partly explain variations in low-oxygen conditions. However, it is also obvious that variability around the best fit is large (Figure 7).

The next question is: What drives variations in the biological rates? Since the annual correlations presented in the previous section indicate that variability in annual FW input partly explains interannual variability in hypoxia, we consider whether FW variability is related to variations in biological rates. Using daily plume extent as a measure of FW presence and comparing it to daily rates of PP, OC, SOC, and bottom oxygen, we find that bottom oxygen and biological rates are significantly correlated with the extent of the FW plume with correlation coefficients ranging from 43% to 62% (Table 1). In other words, variability in the extent of the FW plume explains roughly half of the variability in biological rates. Mechanistically, the presence of a large FW plume not only affects hypoxia by increasing vertical stratification and thus inhibiting vertical supply of oxygen to the subsurface but also because PP and respiration is larger in the plume. Large FW plumes stimulate more widespread biological production and thus oxygen consumption.

Since annual FW input is highly correlated with the extent of the FW plume (see Figure 5g), variability in its extent is partly due to variations in riverine input, but coastal circulation and mixing processes must be playing a role as well. Next, we analyze the impact of the underlying physical drivers.

3.2.3 Physical drivers of short-term variability in hypoxia

Deleted: *intra-seasonal*

We focus our analysis of physical drivers on wind direction and wind strength, and their relation to FW plume location and extent because the latter has already been identified as an explanatory variable for interannual variations in the previous section.

Wind direction is relevant because for most of June, July, and August winds blow predominantly from the south, but switch to predominantly northerly winds between the second half of August and the end of September. As a result of the northward, upwelling favorable winds in the early summer, the FW plume is spread offshore and overlaps primarily with the northern zone. After the switch to mostly southward, downwelling-favorable directions, the FW plume moves southward, becomes more contained near the coast, and grows in its southward extent as it is transported by a coastal current. Wind direction has a demonstrable impact on PP and the extent of the FW plume as shown in Figure 8 for the month of September. Especially in the northern region, PP and plume extent are notably larger during southerly winds when the FW plume is more spread out, than during northerly winds when the plume is more restricted within the coastal current.

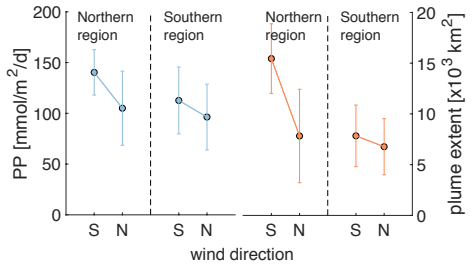

Figure 8. Mean PP and FW plume extent in the northern and southern regions averaged over all days during the 6-yr simulation with north and south wind (i.e. when direction is +/- 45˚ of true north or south) and wind strength >0.03 Pa for in September.

Wind strength is relevant because storm events can erode vertical stratification and thus lead to resupply of oxygen to bottom waters due to vertical mixing. We investigated the effect of wind strength on bottom oxygen, hypoxia, and the extent of the FW plume by first inspecting time series of these variables (Figure S8). We isolated all events during the

433 months June to September and, in Figure 10, show the corresponding changes in wind
434 stress, mean bottom oxygen in the northern and southern zones, and the extent of the FW
435 plume. We diagnosed these events as follows. First, we identified all days when the wind
436 stress exceeded 0.12 Pa. Then we detected the minima in wind stress adjacent to the high-
437 wind days by searching for minima in wind stress within 3 days prior and 3 days after the
438 high-wind days. The periods within these minima are used as analysis period for each wind
439 event. In four instances the wind stress exceeded the threshold within 5 days of a previous
440 wind event. Those subsequent high-wind events were combined into one. We identified
441 the minimum in bottom oxygen (maximum in FW plume area) at the beginning of the event
442 and the maximum in oxygen (minimum in FW area) after the maximum in wind stress was
443 reached.
444 Figure 9a illustrates rapid increases in wind stress typically within 2 to 4 days. The only
445 exceptions are the 4 events where two storms occurred in rapid succession and the
446 combined event lasted longer (up to 8 days) until maximum wind stress was reached. The
447 year with the most wind events is 2013 (with 8 in total including one of the combined long-
448 lasting event). The year with the least events is 2010 (2 events) followed by 2009 (3 events).
449 Most of these events resulted in notable increases in mean bottom oxygen, typically by 10
450 to 30 mmol m^{-3}, but up to 100 mmol m^{-3} in 2010 in the southern zone (Figure 9b). In the
451 rare cases where bottom oxygen did not increase or slightly decreased, bottom oxygen was
452 already elevated before the wind event. The wind events strongly affected the extent of the
453 FW plume (Figure 9c) by mixing the FW layer with underlying ocean water. The effects
454 were largest when the FW plume was most expansive. This analysis shows the significant
455 role of storm events in disrupting the generation of low-oxygen conditions and ventilating
456 bottom waters.

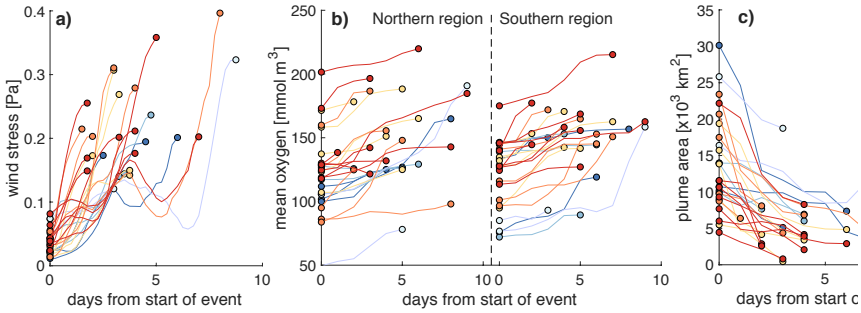

Figure 9. Evolution of a) wind stress, b) bottom mean oxygen in the northern and southern regions, and c) extent of the FW plume during high-wind events. These events are defined by wind stress exceeding 0.12 Pa.

In section 3.2.1 above, where we discussed interannual variability, we noted that while the years 2010 and 2012 had very similar FW input and DIN load, 2010 had a much larger hypoxic area. Likewise, the years 2009 and 2013 were very similar in terms of FW input and DIN load, but 2009 had a much larger hypoxic area. It now becomes obvious that the frequency and severity of high-wind events, i.e. variations on short timescales, explains the interannual differences in both cases.

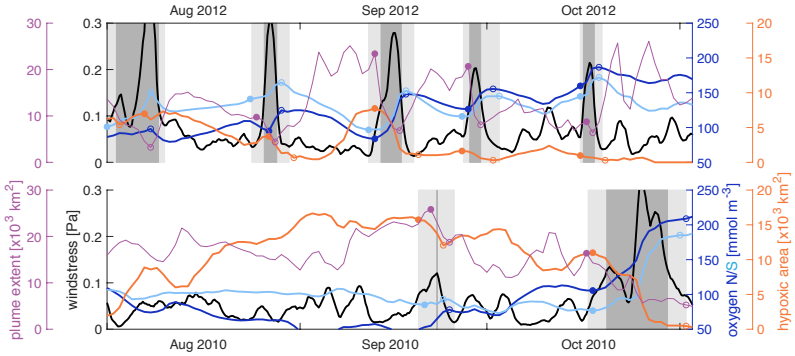

Figure 10. Wind stress (black), mean bottom oxygen in the northern and southern zones (dark and light blue), total hypoxic extent (orange), and FW plume extent (purple) throughout August, September and October of 2010 and 2012. The filled and open circles indicate a variables' value at

472 the beginning and after high-wind events. High-wind days/events are indicated by the dark/light
473 gray shading.
474 Figure 10 shows the wind stress, mean bottom oxygen in the northern and southern
475 zones, and total hypoxic extent and FW plume extent in 2012 and 2010. In 2012, there
476 were 5 high-wind events during the months of August, September, and October that all
477 coincided with increases in bottom oxygen, decreases in hypoxic extent when a hypoxic
478 zone was established at the beginning of the event, and decreases in FW plume extent.
479 Inspection of the evolution of bottom oxygen is especially instructive. While bottom
480 oxygen concentrations declined during periods with average or low wind, they were
481 essentially reset at a much higher level during each wind event. Whenever the FW plume
482 was extensive at the beginning of a high-wind event, it was drastically reduced during the
483 event. In 2010, bottom oxygen was at similar levels to 2012 at the beginning of August but
484 dropped to low levels throughout August, especially in the northern zone, and remained
485 low with widespread hypoxia until a major wind event in the second half of October
486 ventilated bottom waters. Except for a very short event in the second half of September,
487 there were no high-wind events from August until mid-October in 2010.
488 The differences in hypoxia in 2009 and 2013 can also be explained by the frequency and
489 intensity of high-wind events. In 2013, there were 8 high-wind events from July to October
490 that led to an almost continuous ventilation of bottom waters while in 2009 there were only
491 3 such events during the same period (Figure S8). Low to average winds from mid-August
492 to early October of 2009 coincided with a decline in bottom oxygen and establishment of
493 an expansive hypoxic zone throughout most of September.
494 These analyses show that wind direction and strength play an important role in
495 determining the location of the hypoxic zone (i.e. northern versus southern region) and the
496 extent and severity of hypoxic conditions.
497
498 ***3.3 Oxygen budgets for the northern and southern regions***
499 In order to further investigate the roles of physical and biological processes in regulating
500 hypoxia, oxygen budgets were calculated from daily model output for the period from
501 March to November for the northern and southern hypoxic regions. Considering that
502 hypoxic conditions occur near the bottom, we evaluate an oxygen budget not only for the

whole water column but also for its lower portion which typically becomes hypoxic. To account for variations in the thickness of the hypoxic layer, which tends to be thicker in deeper waters (similar to observations by Ning et al., 2011), we include the bottommost 12 layers of our model grid. Because of the model's terrain-following vertical coordinates, the thickness of these 12 model layers varies with total depth. The terms considered in the budget are air-sea flux, lateral physical advection and diffusion, vertical turbulent diffusion (for the subsurface budget only), PP, WOC (including respiration and nitrification), and SOC. Each term was integrated vertically over the whole water column and also over the bottom-most 12 layers and then averaged for the northern and southern regions for each month (Figure 11). We also report these terms for the months during which oxygen decreases (March to August) in Table S2.

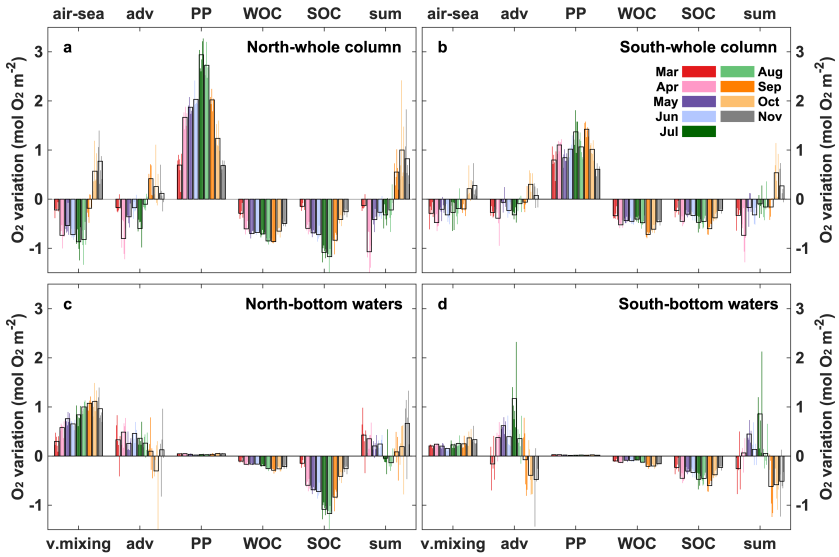

Figure 11. Monthly averaged (2008-2013) oxygen budgets for the whole water column and subsurface water from March to November in the northern and southern hypoxic regions. Adv represents lateral advection and lateral diffusion which is comparatively small, while v.mixing represents vertical turbulent diffusion, which is only relevant for the subsurface budget. Thin color bars represent individual years whereas the black bars are the 6-year average.

For the whole water column (Figure 11a, b), biological processes (PP, WOC, and SOC) greatly exceed physical processes (air-sea exchange and advective transport) in affecting oxygen. PP is always greater than the sum of WOC and SOC in the whole column indicating autotrophy in spring and summer. Advection is negative, acting as an oxygen sink and offsetting 21% of PP on average in the northern and southern regions. Of the two biological oxygen consumption terms (WOC and SOC), WOC accounts for half of total respiration. Negative air-sea flux indicates oxygen outgassing into the atmosphere and is due to photosynthetic oxygen production and decreasing oxygen solubility. However, since hypoxia only occurs in the subsurface, the subsurface budget below is more instructive.

When considering only subsurface waters (Figure 11c, d), the influence of PP decreases markedly, accounting for less than 2% of that in the whole water column. Vertical turbulent

diffusion acts as the largest oxygen source in the subsurface layer. SOC is the dominant oxygen sink accounting for 80% of the total biological oxygen consumption. As photosynthetic oxygen production increases gradually from spring to summer (Figure 12a, b) WOC and SOC also increase as they are closely associated with photosynthetically produced organic matter. Vertical oxygen diffusion tends to covary with PP, implying an oxygen gradient driven by photosynthetic oxygen production in the upper layer. Lateral advection of oxygen is negative in March only (early in the hypoxic season) mainly in the southern region but becomes positive later. This suggests that early in the hypoxic season, import of low-oxygen water contributes to hypoxia generation but advection switches to an oxygen source later. Overall, oxygen sources and sink terms are similar in the northern and southern regions.

4. Discussion

We implemented and validated a state-of-the-art physical-biological model for the ECS. The implementation is based on a model that was previously developed and extensively used for the northern Gulf of Mexico (Fennel et al. 2011, Laurent et al. 2012, Yu at al.2015b), a region that is similar to the ECS in that it receives large inputs of FW and nutrients from a major river and develops extensive, annually recurring hypoxia (see Table 1 in Fennel and Testa (2019). Our model is more comprehensive than previous models for the ECS.

A 6-year simulation was performed and compared to available observations. The model faithfully represents patterns and variability in surface and bottom temperature and salinity, surface chlorophyll and nitrate distributions, bottom oxygen, and correctly simulates the major current patterns in the region (see Section 3.1 and Supplement). We thus deem the model's skill as sufficient for the analysis of biological and physical drivers of hypoxia generation presented here.

The model simulates annually recurring hypoxic conditions but with significant interannual and short-term variability and marked differences in phenology of hypoxic conditions from year to year (Figure 4a, b, c). Interannual variability in hypoxic conditions is much larger than variations in FW input, nutrient load, and bottom oxygen concentrations (Figure 4b) because small variations in oxygen can lead to large changes in

Deleted: intra-seasonal

hypoxic area when bottom oxygen is near the hypoxic threshold. Interannual variability in hypoxic area is partly explained by variations in annual FW input, consistent with previous studies (Zheng et al., 2016; Zhou et al., 2017). While the correlation between time-integrated hypoxic area and FW input is insignificant, there is a strong and significant negative correlation between mean bottom oxygen in August and annual FW input (Figure 5). Annual FW input is also correlated strongly and significantly with the annually integrated spatial extent of the FW plume, which is a useful metric for extent of the region directly influenced by riverine inputs which induce strong density stratification and high productivity.

Surprisingly, DIN load is not correlated with FW input, hypoxic area, and mean bottom oxygen in August (Figure 5). This is in contrast to the northern Gulf of Mexico where DIN load is highly correlated with both FW input and nutrient load and frequently used as a predictor of hypoxic extent (Scavia et al. 2017; Laurent and Fennel 2019). However, the lack of correlation between hypoxia and DIN load in the ECS should not be interpreted as biological processes being unimportant in hypoxia generation, just that variations in DIN load do not explain year-to-year differences. In fact, hypoxic area and biological rates (i.e. mean August PP, OC, and SOC) are strongly and significantly correlated (Figure 5), emphasizing the dominant role of biological oxygen consumption. The fact that riverine variations in DIN load do not seem to have an effect suggests that riverine nutrient inputs are large enough to saturate the region with nutrients, similar to the northern Gulf of Mexico where small reductions in nutrient load have a relatively small effect (Fennel and Laurent 2018).

Variations in riverine FW input only partly explain interannual variations in hypoxia. For example, the years 2010 and 2012 had similar FW inputs and DIN loads but the hypoxic area was 4 times larger in 2010 than 2012 (Figure 5a). Similarly, 2009 and 2013 had the same FW inputs and nutrient loads but 2009 experienced extensive hypoxia while there was almost none in 2013. In order to elucidate these differences, we investigated biological and physical drivers on shorter time scales.

Deleted: of intra-seasonal variability

In the ECS, two distinct zones of low oxygen have been observed (Li et al., 2002; Wei et al., 2007; Zhu et al., 2016, 2011). The model simulates these two zones, referred to as the northern and southern zones, consistent with observations (Figure 4d) and with

589 generally higher PP and SOC in the northern zone (Figure 6). Because of these differences
590 we treated the two zones separately in our analysis of intra-seasonal drivers.
591 We found daily biological rates (i.e. PP, OC, SOC) to be significantly correlated with
592 bottom oxygen in both zones, but with relatively large variability around the best linear fit
593 (Figure 7). The biological rates and bottom oxygen are also significantly correlated with
594 the extent of the FW plume (Table 1). Again, these results emphasize the dominant role of
595 biological oxygen consumption, and its relation to riverine inputs, in hypoxia generation
596 but leave a significant fraction of the variability unexplained.
597 Intra-seasonal variability in hypoxic conditions is significantly related to the extent of
598 the FW plume which is partly explained by variations in riverine FW input but strongly
599 modulated by coastal circulation and mixing. Their influence is elucidated by our analysis
600 of the effects of wind direction and strength on hypoxia. Wind direction has a notable effect
601 on the geographic distribution of hypoxia. Southerly, upwelling-favorable winds lead to a
602 more widespread eastward extension of the FW plume with elevated PP and vertical
603 density stratification (Figure 8). Northerly, downwelling-favorable winds create a coastally
604 trapped southward jet that moves FW southward and constrains the plume close to the coast.
605 A similar behavior has been described for the northern Gulf of Mexico (Feng et al., 2014).
606 Wind strength turned out to be one of the dominant factors in hypoxia evolution. We
607 identified high-wind events and showed that whenever bottom oxygen is low, the
608 occurrence of a high-wind event will lead to a partial reoxygenation of bottom waters and
609 decrease hypoxic extent (Figure 9). The impact of high-wind events is also visible in the
610 extent of the FW plume, which is drastically reduced during high winds because FW is
611 mixed. The frequency of high-wind events during summer explains the interannual
612 differences in hypoxic area between 2010 and 2012 (Figure 10) and 2009 and 2013 (Figure
613 S8). In 2009 and 2010 there were only few high-wind events during summer while 2012
614 and 2013 experienced a sequence of storms that led to partial reoxygenation of the water
615 column throughout the summer and thus impeded the development hypoxia.
616 We calculated oxygen budgets for the northern and southern regions considering the
617 whole water-column and the near-bottom layer only. The subsurface budget is particularly
618 useful in providing insights into when and where lateral advection amplifies or mitigates
619 hypoxia and illustrates that SOC is the dominant oxygen sink in the subsurface. The relative

importance of WOC and SOC had not previously been quantified for this region due to lack of concurrent WOC and SOC observations and lack of models that realistically account for both processes. The budget for the whole water column is less useful because it is dominated by the oxygen sources, sinks and transport in the surface layer, which does not experience hypoxia and thus is not relevant.

The importance of SOC suggested by our model is consistent with recent observational studies in the ECS. SOC on the coastal shelves in the Yellow Sea and ECS has been estimated to range from 1.7 to 17.6 mmol O_2 m^{-2} d^{-1} (mean rate of 7.2 mmol O_2 m^{-2} d^{-1}) from April to October except August by Song et al. (2016), and from 9.1 to 62.5 mmol O_2 m^{-2} d^{-1} (mean of 22.6±16.4 mmol O_2 m^{-2} d^{-1}) from June to October in Zhang et al. (2017). Simulated SOC in the typical low-oxygen zone falls within the range observed by Zhang et al. (2017) with a mean rate of 20.6±19.2 mmol O_2 m^{-2} d^{-1} between April and October. Based on observations, Zhang et al. (2017) already suggested that SOC is a major contributor to hypoxia formation in below-pycnocline waters, which is further corroborated by our model results. It is also consistent with the modelling study of Zhou et al. (2017), who did not include SOC in the baseline version of their model but showed in a sensitivity study that inclusion of SOC simulates hypoxic extent more realistically. Our results are in line with findings from the northern Gulf of Mexico hypoxic zone where WOC is much larger than SOC below the pycnocline, while SOC is dominant in the bottom 5 m where hypoxia occurs most frequently in summer (Quiñones-Rivera et al., 2007; Yu et al., 2015b).

The finding that lateral oxygen transport can act as a net source to subsurface water is also new. On seasonal scales, oxygen advection in the subsurface varies from an oxygen sink in spring to a source in summer, especially in the southern hypoxic region, implying that the TWC becomes an oxygen source when oxygen is depleted in the hypoxic region. This aspect was neglected in previous studies which only emphasized the role of advection as an oxygen sink promoting hypoxia formation (Ning et al., 2011; Qian et al., 2015). The Taiwan Warm Current originates from the subsurface of the Kuroshio northeast to Taiwan Island, and thus represents an intrusion onto the continental shelves from the open ocean (Guo et al., 2006). In addition to oxygen advection, nutrients are transported supporting PP on the ECS shelves (Zhao & Guo, 2011; Grosse et al., 2020). The intrusion of the Taiwan Warm Current and the Kuroshio accompanied by relatively cold and saline water, and

Deleted: in

652 nutrient and oxygen transport, is thought to influence hypoxia development (Li et al., 2002;
653 Wang, 2009; Zhou et al., 2017) but no quantification of the relative importance has
654 occurred until now (see companion paper by Grosse et al., 2020, using the same model).
655
656 **5. Conclusions**
657 In this study, a new 3D coupled physical-biological model for the ECS was presented
658 and used to explore the spatial and temporal evolution of hypoxia off the CE and to quantify
659 the major processes controlling interannual and intra-seasonal oxygen dynamics.
660 Validation shows that the model reproduces the observed spatial distribution and temporal
661 evolution of physical and biological variables well.
662 A 6-year simulation with realistic forcing produced large interannual and intra-seasonal
663 variability in hypoxic extent despite relatively modest variations in FW input and nutrient
664 loads. The interannual variations are partly explained by variations in FW input but not
665 DIN load. Nevertheless, elevated rates of biological oxygen consumption are of paramount
666 importance for hypoxia generation in this region, as shown by the high correlation between
667 hypoxic area, bottom oxygen, and biological rates (PP, OC, SOC) on both annual and
668 shorter time scales.
669 Other important explanatory variables of variability in hypoxia are wind direction and
670 strength. Wind direction affects the magnitude of PP and the spatial extent of the FW plume,
671 because southerly, upwelling favorable winds tend to spread the plume over a large area
672 while northerly, downwelling-favorable winds push the plume against the coast and induce
673 a coastal current that contains the FW and moves it downcoast. Wind strength is important
674 because high-wind events lead to a partial reoxygenation whenever bottom oxygen is low
675 and can dramatically decrease the extent of the FW plume. The frequency of high-wind
676 events explains some of the interannual differences in hypoxia, where years with similar
677 FW input, nutrient load, and mean rates of oxygen consumption display very different
678 hypoxic extents because high-wind events lead to partial reoxygenation of bottom waters.
679 A model-derived oxygen budget shows that SOC is larger than WOC in the subsurface
680 of the hypoxic region. Lateral advection of oxygen in the subsurface switches from an
681 oxygen sink in spring to a source in summer especially in the southern region and is likely

Deleted: have

associated with open-ocean intrusions onto the coastal shelf supplied by the Taiwan Warm Current.

Acknowledgments: HZ was supported by the National Key Research and Development Program of China (2016YFC1401602 and 2017YFC1404403) and the China Scholarship Council (CSC). The authors thank the crew of the Dongfanghong2 for providing much help during the sampling cruises, and Compute Canada for access to supercomputer time. KF acknowledges support from the NSERC Discovery Program.

Code/Data Availability: The ROMS model code is available at http://myroms.org. NOAA AVHRR and MODIS-Terra are available at https://www.nodc.noaa.gov/SatelliteData/ghrsst/ and http://oceancolor.gsfc.nasa.gov/. The model results are available on request to the authors.

Author Contributions: The manuscript is based on HZ's PhD thesis (in Chinese). CB implemented the physical model. HZ added the biological component, performed model simulations, and wrote the first version of the manuscript with input from KF and AL. For the manuscript revision, AL reran the model simulation, AL and KF performed additional analyses, and KF revised the text with input from all co-authors.

Competing Interests: The authors declare they have no competing interests.

References

Baird, D., Christian, R. R., Peterson, C. H., & Johnson, G. A.: Consequences of hypoxia on estuarine ecosystem function: Energy diversion from consumers to microbes. Ecological Applications, 14(3), 805–822. https://doi.org/10.1890/02-5094, 2004.

Bian, C., Jiang, W., & Greatbatch, R. J.: An exploratory model study of sediment transport sources and deposits in the Bohai Sea, Yellow Sea, and East China Sea. Journal of Geophysical Research: Oceans, 118(11), 5908–5923. https://doi.org/10.1002/2013JC009116, 2013a.

Bian, C., Jiang, W., Quan, Q., Wang, T., Greatbatch, R. J., & Li, W.: Distributions of suspended sediment concentration in the Yellow Sea and the East China Sea based on field surveys during the four seasons of 2011. Journal of Marine Systems, *121–122*, 24–35, https://doi.org/10.1016/j.jmarsys.2013.03.013, 2013b.

Bianchi, T. S., DiMarco, S. F., Cowan, J. H., Hetland, R. D., Chapman, P., Day, J. W., & Allison, M. A.: The science of hypoxia in the northern Gulf of Mexico: A review. Science of the Total Environment, 408(7), 1471–1484. https://doi.org/10.1016/j.scitotenv.2009.11.047, 2010.

715 Bishop, M. J., Powers, S. P., Porter, H. J., & Peterson, C. H.: Benthic biological effects of
716 seasonal hypoxia in a eutrophic estuary predate rapid coastal development. Estuarine, Coastal
717 and Shelf Science, 70(3), 415–422. https://doi.org/10.1016/j.ecss.2006.06.031, 2006.
718 Capet, A., Beckers, J. M., & Grégoire, M.: Drivers, mechanisms and long-term variability of
719 seasonal hypoxia on the Black Sea northwestern shelf - Is there any recovery after
720 eutrophication? Biogeosciences, 10(6), 3943–3962. https://doi.org/10.5194/bg-10-3943-2013,
721 2013.
722 Carton, J. A., & Giese, B. S.: A Reanalysis of Ocean Climate Using Simple Ocean Data
723 Assimilation (SODA). Monthly Weather Review, 136(8), 2999–3017,
724 https://doi.org/10.1175/2007MWR1978.1, 2008.
725 Chen, C. C., Gong, G. C., & Shiah, F. K., Hypoxia in the East China Sea: One of the largest
726 coastal low-oxygen areas in the world. Marine Environmental Research, 64(4), 399–408.
727 https://doi.org/10.1016/j.marenvres.2007.01.007, 2007.
728 Chen, J., Cui, T., Ishizaka, J., & Lin, C.: A neural network model for remote sensing of diffuse
729 attenuation coefficient in global oceanic and coastal waters: Exemplifying the applicability of
730 the model to the coastal regions in Eastern China Seas. Remote Sensing of Environment, *148*,
731 168–177. https://doi.org/10.1016/j.rse.2014.02.019, 2014.
732 Chen, X., Shen, Z., Li, Y., & Yang, Y.: Physical controls of hypoxia in waters adjacent to the
733 Yangtze Estuary: A numerical modeling study. Marine Pollution Bulletin, *97*(1–2), 349–364.
734 https://doi.org/10.1016/j.marpolbul.2015.05.067, 2015a.
735 Chen, X., Shen, Z., Li, Y., & Yang, Y.: Tidal modulation of the hypoxia adjacent to the Yangtze
736 Estuary in summer. Marine Pollution Bulletin, *100*(1), 453–463,
737 https://doi.org/10.1016/j.marpolbul.2015.08.005, 2015b.
738 Dee, D. P., Uppala, S. M., Simmons, A. J., Berrisford, P., Poli, P., Kobayashi, S., … Vitart, F.:
739 The ERA-Interim reanalysis: Configuration and performance of the data assimilation system.
740 Quarterly Journal of the Royal Meteorological Society, *137*(656), 553–597.
741 https://doi.org/10.1002/qj.828, 2011.
742 Diaz, R. J., & Rosenberg, R.: Spreading dead zones and consequences for marine ecosystems.
743 Science, *321*(5891), 926–929. https://doi.org/10.1126/science.1156401, 2008.
744 Egbert, G. D., & Erofeeva, S. Y.: Efficient inverse modeling of barotropic ocean tides. Journal of
745 Atmospheric and Oceanic Technology, *19*(2), 183–204. https://doi.org/10.1175/1520-
746 0426(2002)019<0183:EIMOBO>2.0.CO;2, 2002.

747 Feng, Y., Fennel, K., Jackson, G.A., DiMarco, S.F. & Hetland, R.D.: A model study of the
748 response of hypoxia to upwelling favorable wind on the northern Gulf of Mexico shelf, Journal
749 of Marine Systems 131, 63-73, 2014.
750 Fennel, K., and Testa, J.M.: Biogeochemical controls on coastal hypoxia, Annual Review of
751 Marine Science, 11, 105-130, https://doi.org/10.1146/annurev-marine-010318-095138, 2019.
752 Fennel, K. and Laurent, A.: N and P as ultimate and proximate limiting nutrients in the northern
753 Gulf of Mexico: implications for hypoxia reduction strategies, Biogeosciences, 15, 3121-3131,
754 https://doi.org/ /10.5194/bg-15-3121-2018, 2018.
755 Fennel, K., Hetland, R., Feng, Y., & DiMarco, S.: A coupled physical-biological model of the
756 Northern Gulf of Mexico shelf: Model description, validation and analysis of phytoplankton
757 variability. Biogeosciences, *8*(7), 1881–1899. https://doi.org/10.5194/bg-8-1881-2011, 2011.
758 Fennel, K., Hu, J., Laurent, A., Marta-Almeida, M., & Hetland, R.: Sensitivity of hypoxia
759 predictions for the northern Gulf of Mexico to sediment oxygen consumption and model
760 nesting. Journal of Geophysical Research: Oceans, *118*(2), 990–1002.
761 https://doi.org/10.1002/jgrc.20077, 2013.
762 Fennel, K., Wilkin, J., Levin, J., Moisan, J., O'Reilly, J., & Haidvogel, D.: Nitrogen cycling in
763 the Middle Atlantic Bight: Results from a three-dimensional model and implications for the
764 North Atlantic nitrogen budget. Global Biogeochemical Cycles, *20*(3), 1–14.
765 https://doi.org/10.1029/2005GB002456, 2006.
766 Garcia, H. E., Boyer, T. P., Locarnini, R. A., Antonov, J. I., Mishonov, A. V, Baranova, O. K., …
767 Johnson, D. R.: World Ocean Atlas 2013. Volume 3: dissolved oxygen, apparent oxygen
768 utilization, and oxygen saturation. NOAA Atlas NESDIS 75, 2013a.
769 Garcia, H. E., Locarnini, R. A., Boyer, T. P., Antonov, J. I., Baranova, O. K., Zweng, M. M., …
770 Johnson, D. R.: World Ocean Atlas 2013, Volume 4 : Dissolved Inorganic Nutrients
771 (phosphate, nitrate, silicate). NOAA Atlas NESDIS 76 (Vol. 4), 2013b.
772 Grosse, F., Fennel, K., Zhang, H., Laurent, A.: Quantifying the contributions of riverine vs.
773 oceanic nitrogen to hypoxia in the East China Sea, Biogeosciences, https://doi.org/10.5194/bg-
774 2019-342, accepted for publication
775 Guo, J. S., X. M. Hu and Y. L. Yuan: A diagnostic analysis of variations in volume transport
776 through the Taiwan Strait using satellite altimeter data, Advances in Marine Science, 23(1):
777 20 – 26 (in Chinese with English abstract), 2005.
778 Haidvogel, D. B., Arango, H., Budgell, W. P., Cornuelle, B. D., Curchitser, E., Di Lorenzo, E., …
779 Wilkin, J., Ocean forecasting in terrain-following coordinates: Formulation and skill

780 assessment of the Regional Ocean Modeling System. Journal of Computational Physics,
781 227(7), 3595–3624. https://doi.org/10.1016/j.jcp.2007.06.016, 2008.
782 Laurent, A., & Fennel, K.: Simulated reduction of hypoxia in the northern Gulf of Mexico due to
783 phosphorus limitation. Elementa: Science of the Anthropocene, *2*(1), 000022.
784 https://doi.org/10.12952/journal.elementa.000022, 2014.
785 Laurent, A., Fennel, K.: Time-evolving, spatially explicit forecasts of the northern Gulf of
786 Mexico hypoxic zone. Environmental Science & Technology, 53, 14,449-14,458, doi:
787 10.1021/acs.est.9b05790, 2019.
788 Laurent, A., Fennel, K., Hu, J., & Hetland, R.: Simulating the effects of phosphorus limitation in
789 the Mississippi and Atchafalaya river plumes. Biogeosciences, *9*(11), 4707–4723.
790 https://doi.org/10.5194/bg-9-4707-2012, 2012.
791 Laurent, A., Fennel, K., Cai, W.-J., Huang, W.-J., Barbero, L., Wanninkhof, R.: Eutrophication-
792 Induced Acidification of Coastal Waters in the Northern Gulf of Mexico: Insights into Origin
793 and Processes from a Coupled Physical-Biogeochemical Model. Geophys. Res. Lett., *44* (2),
794 946–956. https://doi.org/10.1002/2016GL071881, 2017.
795 Li, D., Zhang, J., Huang, D., Wu, Y., & Liang, J.: Oxygen depletion off the Changjiang (Yangtze
796 River) Estuary. Science in China Series D: Earth Science, *45*(12), 1137.
797 https://doi.org/10.1360/02yd9110, 2002.
798 Li, H. M., Tang, H. J., Shi, X. Y., Zhang, C. S., & Wang, X. L.: Increased nutrient loads from the
799 Changjiang (Yangtze) River have led to increased Harmful Algal Blooms. Harmful Algae, *39*,
800 92–101. https://doi.org/10.1016/j.hal.2014.07.002, 2014.
801 Li, M., Lee, Y. J., Testa, J. M., Li, Y., Ni, W., Kemp, W. M., & Di Toro, D. M.: What drives
802 interannual variability of hypoxia in Chesapeake Bay: Climate forcing versus nutrient loading?
803 Geophysical Research Letters, *43*(5), 2127–2134. https://doi.org/10.1002/2015GL067334,
804 2016.
805 Li, X., Bianchi, T. S., Yang, Z., Osterman, L. E., Allison, M. A., DiMarco, S. F., & Yang, G.:
806 Historical trends of hypoxia in Changjiang River estuary: Applications of chemical biomarkers
807 and microfossils. Journal of Marine Systems, *86*(3–4), 57–68, 2011.
808 https://doi.org/10.1016/j.jmarsys.2011.02.003
809 Liu, K. K., Yan, W., Lee, H. J., Chao, S. Y., Gong, G. C., & Yeh, T. Y.: Impacts of increasing
810 dissolved inorganic nitrogen discharged from Changjiang on primary production and seafloor
811 oxygen demand in the East China Sea from 1970 to 2002. *Journal of Marine Systems*, *141*,
812 200–217. https://doi.org/10.1016/j.jmarsys.2014.07.022, 2015.

Liu, S. M., Hong, G.-H., Ye, X. W., Zhang, J., & Jiang, X. L.: Nutrient budgets for large Chinese estuaries and embayment. Biogeosciences Discussions, *6*(1), 391–435. https://doi.org/10.5194/bgd-6-391-2009, 2009.

Liu, S. M., Zhang, J., Chen, H. T., Wu, Y., Xiong, H., & Zhang, Z. F.: Nutrients in the Changjiang and its tributaries. Biogeochemistry, *62*(1), 1–18, 2003.

Locarnini, R. A., Mishonov, A. V., Antonov, J. I., Boyer, T. P., Garcia, H. E., Baranova, O. K., … Seidov, D.: World Ocean Atlas 2013. Vol. 1: Temperature. S. Levitus, Ed.; A. Mishonov, Technical Ed.; NOAA Atlas NESDIS, 73, 40. https://doi.org/10.1182/blood-2011-06-357442, 2013.

Ni, X., Huang, D., Zeng, D., Zhang, T., Li, H., & Chen, J.: The impact of wind mixing on the variation of bottom dissolved oxygen off the Changjiang Estuary during summer. Journal of Marine Systems, 154, 122–130. https://doi.org/10.1016/j.jmarsys.2014.11.010, 2016.

Ning, X., Lin, C., Su, J., Liu, C., Hao, Q., & Le, F.: Long-term changes of dissolved oxygen, hypoxia, and the responses of the ecosystems in the East China Sea from 1975 to 1995. Journal of Oceanography, 67(1), 59–75. https://doi.org/10.1007/s10872-011-0006-7, 2011.

Peña, A., Katsev, S., Oguz, T., & Gilbert, D.: Modeling dissolved oxygen dynamics and hypoxia. Biogeosciences, *7*(3), 933–957. https://doi.org/10.5194/bg-7-933-2010, 2010.

Qian, W., Dai, M., Xu, M., Kao, S. ji, Du, C., Liu, J., … Wang, L.: Non-local drivers of the summer hypoxia in the East China Sea off the Changjiang Estuary. Estuarine, Coastal and Shelf Science, 1–7. https://doi.org/10.1016/j.ecss.2016.08.032, 2015.

Quiñones-Rivera, Z. J., Wissel, B., Justić, D., & Fry, B.: Partitioning oxygen sources and sinks in a stratified, eutrophic coastal ecosystem using stable oxygen isotopes. Marine Ecology Progress Series, *342*, 69–83. https://doi.org/10.3354/meps342069, 2007.

Rabalais, N. N., Díaz, R. J., Levin, L. A., Turner, R. E., Gilbert, D., & Zhang, J.: Dynamics and distribution of natural and human-caused hypoxia. Biogeosciences, *7*, 585–619. https://doi.org/10.5194/bg-7-585-2010, 2010.

Scavia, D., Bertani, I., Obenour, D. R., Turner, R. E., Forrest, D. R. & Katin, A.: Ensemble modeling informs hypoxia management in the northern Gulf of Mexico, P. Natl. Acad. Sci. USA, 114, 8823–8828, 2017.

Scully, M. E.: Physical controls on hypoxia in Chesapeake Bay: A numerical modeling study. Journal of Geophysical Research: Oceans, *118*(3), 1239–1256, https://doi.org/10.1002/jgrc.20138, 2013.

Smolarkiewicz, P. K., & Margolin, L. G.: MPDATA: A finite-difference solver for geophysical flows. Journal of Computational Physics, 140, 459-480, 1998.

847 Song, G., Liu, S., Zhu, Z., Zhai, W., Zhu, C., & Zhang, J.: Sediment oxygen consumption and
848 benthic organic carbon mineralization on the continental shelves of the East China Sea and the
849 Yellow Sea. Deep-Sea Research Part II: Topical Studies in Oceanography, *124*, 53–63.
850 https://doi.org/10.1016/j.dsr2.2015.04.012, 2016.
851 Tong, Y., Zhao, Y., Zhen, G., Chi, J., Liu, X., Lu, Y., … Zhang, W.: Nutrient Loads Flowing into
852 Coastal Waters from the Main Rivers of China (2006–2012). Scientific Reports, *5*, 16678.
853 https://doi.org/10.1038/srep16678, 2015.
854 Umlauf, L., & Burchard, H.: A generic length-scale equation for geophysical. Journal of Marine
855 Research, *61*(2), 235–265. https://doi.org/10.1357/002224003322005087, 2003.
856 Wang, B.: Hydromorphological mechanisms leading to hypoxia off the Changjiang estuary.
857 Marine Environmental Research, 67(1), 53–58,
858 https://doi.org/10.1016/j.marenvres.2008.11.001, 2009.
859 Wang, B., Wei, Q., Chen, J., & Xie, L.: Annual cycle of hypoxia off the Changjiang (Yangtze
860 River) Estuary. Marine Environmental Research, *77*, 1–5,
861 https://doi.org/10.1016/j.marenvres.2011.12.007, 2012.
862 Wang, B., Chen, J., Jin, H., Li, H., Huang, D., & Cai, W.-J.: Diatom bloom-derived bottom water
863 hypoxia off the Changjiang Estuary, with and without typhoon influence, Limnology and
864 Oceanography, 62, 1552-1569, https://doi.org/10.1002/lno.10517, 2017.
865 Wang, H., Dai, M., Liu, J., Kao, S. J., Zhang, C., Cai, W. J., … Sun, Z.: Eutrophication-Driven
866 Hypoxia in the East China Sea off the Changjiang Estuary. Environmental Science and
867 Technology, 50(5), 2255–2263. https://doi.org/10.1021/acs.est.5b06211, 2016.
868 Wang, J., Yan, W., Chen, N., Li, X., & Liu, L.: Modeled long-term changes of DIN:DIP ratio in
869 the Changjiang River in relation to Chl-α and DO concentrations in adjacent estuary. Estuarine,
870 Coastal and Shelf Science, *166*, 153–160. https://doi.org/10.1016/j.ecss.2014.11.028, 2015.
871 Wei, H., He, Y., Li, Q., Liu, Z., & Wang, H.: Summer hypoxia adjacent to the Changjiang
872 Estuary. Journal of Marine Systems, 67(3–4), 292–303,
873 https://doi.org/10.1016/j.jmarsys.2006.04.014, 2007.
874 Wei, H., Luo, X., Zhao, Y., & Zhao, L.: Intraseasonal variation in the salinity of the Yellow and
875 East China Seas in the summers of 2011, 2012, and 2013. Hydrobiologia, *754*(1), 13–28.
876 https://doi.org/10.1007/s10750-014-2133-9, 2015.
877 Wu, R. S. S.: Hypoxia: From molecular responses to ecosystem responses. Marine Pollution
878 Bulletin, *45*(1–12), 35–45. https://doi.org/10.1016/S0025-326X(02)00061-9, 2002.

879 Yu, L., Fennel, K., & Laurent, A.: A modeling study of physical controls on hypoxia generation
880 in the northern Gulf of Mexico. Journal of Geophysical Research C: Oceans, *120*(7), 5019–
881 5039. https://doi.org/10.1002/2014JC010634, 2015a.
882 Yu, L., Fennel, K., Laurent, A., Murrell, M. C., & Lehrter, J. C.: Numerical analysis of the
883 primary processes controlling oxygen dynamics on the Louisiana shelf. Biogeosciences, *12*(7),
884 2063–2076. https://doi.org/10.5194/bg-12-2063-2015, 2015b.
885 Yuan, D., Zhu, J., Li, C., & Hu, D.: Cross-shelf circulation in the Yellow and East China Seas
886 indicated by MODIS satellite observations. Journal of Marine Systems, *70*(1–2), 134–149.
887 https://doi.org/10.1016/j.jmarsys.2007.04.002, 2008.
888 Zhang, H., Zhao, L., Sun, Y., Wang, J., & Wei, H.: Contribution of sediment oxygen demand to
889 hypoxia development off the Changjiang Estuary. Estuarine, Coastal and Shelf Science, 192,
890 149–157. https://doi.org/10.1016/j.ecss.2017.05.006, 2017.
891 Zhang, J.: Nutrient elements in large Chinese estuaries. Continental Shelf Research, *16*(8), 1023–
892 1045. https://doi.org/10.1016/0278-4343(95)00055-0, 1996.
893 Zhao, L., & Guo, X.: Influence of cross-shelf water transport on nutrients and phytoplankton in
894 the East China Sea: A model study. Ocean Science, *7*(1), 27–43. https://doi.org/10.5194/os-7-
895 27-2011, 2011.
896 Zheng, J., Gao, S., Liu, G., Wang, H., & Zhu, X.: Modeling the impact of river discharge and
897 wind on the hypoxia off Yangtze Estuary. Natural Hazards and Earth System Sciences, 16(12),
898 2559–2576. https://doi.org/10.5194/nhess-16-2559-2016, 2016.
899 Zhou, F., Chai, F., Huang, D., Xue, H., Chen, J., Xiu, P., … Wang, K.: Investigation of hypoxia
900 off the Changjiang Estuary using a coupled model of ROMS-CoSiNE. Progress in
901 Oceanography, 159, 237–254. https://doi.org/10.1016/j.pocean.2017.10.008, 2017.
902 Zhou, F., Huang, D., Ni, X., Xuan, J., Zhang, J., & Zhu, K.: Hydrographic analysis on the multi-
903 time scale variability of hypoxia adjacent to the Changjiang River Estuary. Shengtai Xuebao/
904 Acta Ecologica Sinica, 30(17), 4728–4740, 2010.
905 Zhu, J., Zhu, Z., Lin, J., Wu, H., & Zhang, J.: Distribution of hypoxia and pycnocline off the
906 Changjiang Estuary, China. Journal of Marine Systems, *154*, 28–40.
907 https://doi.org/10.1016/j.jmarsys.2015.05.002, 2016.
908 Zhu, Z.-Y., Zhang, J., Wu, Y., Zhang, Y.-Y., Lin, J., & Liu, S.-M.: Hypoxia off the Changjiang
909 (Yangtze River) Estuary: Oxygen depletion and organic matter decomposition. *Marine*
910 *Chemistry*, *125*(1–4), 108–116. https://doi.org/10.1016/j.marchem.2011.03.005, 2011.

Zweng, M. M., Reagan, J. R., Antonov, J. I., Mishonov, A. V., Boyer, T. P., Garcia, H. E., … Bidlle, M. M., World Ocean Atlas 2013, Volume 2: Salinity. NOAA Atlas NESDIS (Vol. 119). https://doi.org/10.1182/blood-2011-06-357442, 2013.